Philosophical Magazine Letters

Critical nuclei and crystallization in colloidal suspensions

H. Löwen [a]; C. N. Likos [a]; L. Assoud [a]; R. Blaak [a]; S. Van Teefelen [a]
[a] Institut für Theoretische Physik II: Weiche Materie, Heinrich-Heine-Universität Düsseldorf, Universitätsstraße 1, Düsseldorf, D-40225, Germany

PLEASE SCROLL DOWN FOR ARTICLE

Critical nuclei and crystallization in colloidal suspensions

H. LÖWEN*, C. N. LIKOS, L. ASSOUD, R. BLAAK and S. VAN TEEFELEN

Institut für Theoretische Physik II: Weiche Materie, Heinrich-Heine-Universität
Düsseldorf, Universitätsstraße 1, D-40225, Düsseldorf, Germany

The aim of this paper is to review and to preview some selected topics of crystal nucleation in colloidal suspensions. First we discuss how the structure of critical nuclei can be calculated by computer simulations, in particular how linear shear flow affects the size and shape of the critical nuclei. Second, we preview the possibilities to access heterogeneous crystal nucleation and dynamics of a crystal by using the recently developed formalism of dynamical density functional theory. In particular, data for global crystal heating are presented.

1. Introduction

The theoretical prediction of crystal nucleation phenomena is an active and still open area of current research [1]. Classical nucleation theory (CNT) is based on the simple thermodynamical consideration of a spherical nucleus covered by a solid–liquid interface which separates the stable crystal phase inside the nucleus from the unstable liquid phase outside. The classical nucleation theory makes explicit predictions for the nucleation rate and the size of the critical nucleus. If the latter is exceeded, growth of the crystallite initiated by the nucleus takes place.

Recently, computer simulation techniques have been applied to extract the size and shape of a critical nucleus in the undercooled melt [2] using the umbrella sampling technique. It was found that the critical nucleus possesses a pretty rough interface and is not spherical in general. The same result has also been extracted from real-space experiments on colloidal suspensions [3].

Very recently a microscopic dynamical theory [4, 5] was put forward to describe crystal nucleation which is a dynamical analogue of the traditional classical density functional theory of freezing [6]. This theory was justified on the basis of the Smoluchowski equation for Brownian systems and allows for a fit-parameter-free description of one-particle density dynamics. This theory can easily be used to describe the deterministic crystal growth once a heterogeneous nucleus of fixed seed particle is offered to the undercooled melt. This can be experimentally realized in colloidal suspensions [7].

*Corresponding author. Email: hlowen@thphy.uni-duesseldorf.de

The aim of this paper is twofold: first, we shall review what is known about the critical nucleus in sheared colloidal suspensions. Here computer simulations have been used in a non-equilibrium situation to access the size and shape of the critical nucleus and its orientation relative to the shear flow. A convenient generalization of classical nucleation theory including a finite shear rate $\dot{\gamma}$ does describe the data surprisingly well although there is a priori no reason for it to work in non-equilibrium. Second, we shall briefly introduce and describe dynamical density functional theory. We apply it to a situation of gradual and rapid global heating of a bulk solid. The relation to the recently proposed phase-field crystal is also briefly discussed.

2. Homogeneous nucleation of colloidal melts under shear

A model colloidal mixture consisting of a Yukawa fluid which performs Brownian motion at fixed temperature was extensively studied by computer simulations [8, 9]. A linear shear flow was imposed† such that a fixed shear rate $\dot{\gamma}$ is prescribed. By generalizing the umbrella sampling technique to non-equilibrium situations [10], the size and shape of the critical crystal nucleus is obtained for different shear rates and 'undercoolings'; the meaning of the latter can be rationalized by the pressure difference to the fluid–solid coexistence pressure.

Results are shown in figure 1 where the number of colloidal particles N^* belonging to the critical cluster is shown as a function of the reduced shear rate $\dot{\gamma}/\kappa^2 D$. Here κ denotes the inverse screening length of the Yukawa interaction and D is the free diffusion constant of the colloidal particles. Data are presented for three different pressures P measured in terms of κ^3/β where β is the inverse thermal energy. The cluster size increases with shear rate. At the same time, the crystallization rate decreases. This implies that shear suppresses crystallization for this particular model. Although classical nucleation theory does not hold a priori in non-equilibrium situations (such as shear), it is tempting to test an ansatz where the shear rate is treated as a thermodynamic variable. Surprisingly good agreement is found, see again the parabolic fits in figure 1, when the concept of classical nucleation theory is applied.

The anisotropy of the critical nucleus relative to the shear flow direction is shown in figure 2. It is tilted relative to the shear gradient direction (y axis). The averaged tilt angle scales linearly with the shear rate, which is the simplest scaling possible compatible with inversion symmetry.

A detailed comparison with experiments is in principle possible.‡ Data for crystallization rates in charged suspensions are known [12] and individual particles can be tracked and visualized under shear flow [13-16]. Still the size of the critical nucleus should be measured, by, e.g. confocal microscopy [3], in order to verify the simulation predictions of [8, 9].

---

† A parabolic Poiseuille flow could in principle also be considered within Brownian dynamics simulations.

‡ First experiments on nucleation under shear were reported in [11].
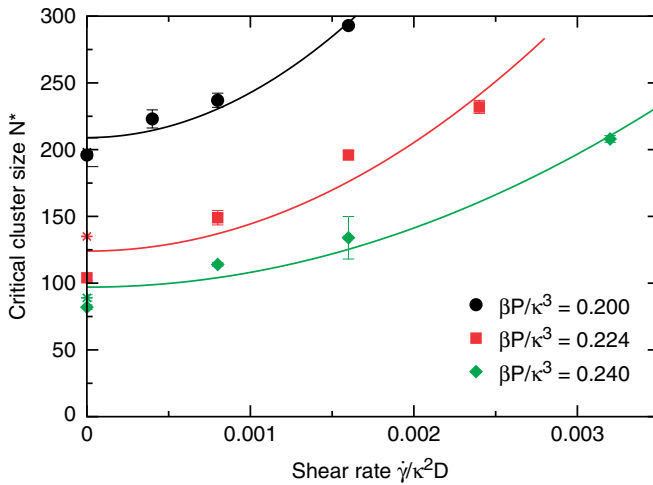
Figure 1. The number of particles N^* of the critical nucleus as a function of the dimensionless shear rate $\dot{\gamma}/\kappa^2 D$ and for different pressures P. The solid lines are parabolic fits through the data. The stars are data from equilibrium Monte Carlo simulations without shear [9].
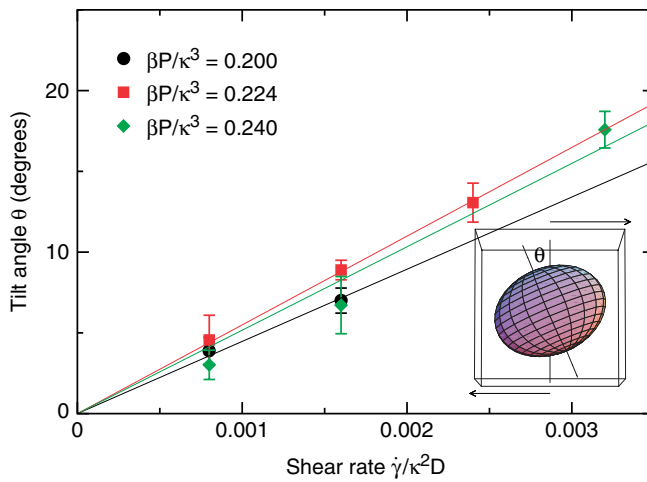
Figure 2. The tilt angle θ of the principal moment of inertia with respect to the y-axis. The inset shows a schematic representation of the preferred orientation of the nucleus with respect to the shear direction indicated by the arrows [8].

3. Dynamical density functional theory

Dynamical density functional theory is the generalization of classical density functional theory which is formulated in terms of the static one-particle density field $\rho(\vec{r})$ towards an *ensemble*-averaged time-dependent one-particle density field $\rho(\vec{r}, t)$.

In the static case [6, 17, 18], a free-energy functional $F[\rho(\vec{r}, t)]$ is uniquely defined. The dynamical generalization can be derived from Smoluchowski's approach [19]. The only assumption is that pair correlations in non-equilibrium are replaced by their corresponding equilibrium expression, an assumption whose validity is amply confirmed by extended studies [23–25]. Then the following dynamical equation for $\rho(\vec{r}, t)$ is derived:

$$\frac{\partial \rho(\vec{r}, t)}{\partial t} = \beta D \vec{\nabla} \cdot \left(\rho(\vec{r}, t) \vec{\nabla} \frac{\delta F[\rho(\vec{r}, t)]}{\delta \rho(\vec{r}, t)} \right). \tag{1}$$

This is a deterministic equation without noise (see the comment of [20]) which is microscopic in principle since all molecular correlations are included in the functional $F[\rho(\vec{r}, t)]$. Note that the mobility coefficient βD is not a phenomenological fit parameter (as typically for order parameter dynamics) but has a precise microscopic meaning. Three remarks are in order: (i) The uniqueness proof of the dynamical functional can be performed also for dynamical density functional theory, see [21]. (ii) Mode coupling theory can be brought into relation with dynamical density functional theory, see [22]. (iii) There are alternative ways of deriving dynamical density functional theory on microscopic grounds [4, 5].

The dynamical density functional theory has been tested against Brownian dynamics computer simulations for strongly inhomogeneous fluids and very good agreement has been found, see e.g. [23, 24]. Hence it is tempting to use the dynamical density functional approach also for crystallization. The conventional static density functional theory provides a microscopic approach to freezing. For a given particle interaction, it is in principle possible to predict the full phase diagram of the system including freezing and melting. The inhomogeneous density profile of the crystal consists of periodic peaks around the solid lattice positions. For a functional $F[\rho(\vec{r}, t)]$ which predicts freezing, the full dynamics of a crystal out of a given starting density profile can then be predicted. Since the dynamical density functional theory works well for strongly inhomogeneous liquids it is expected that it describes the dynamics of freezing as well.

The following problems of heterogeneous nucleation and microstructure formation can be addressed, at least in principle:

(1) Heterogeneous nucleation at an external planar wall, e.g. by a system boundary.
(2) Crystal growth out of an undercooled melt if a piece of crystal with a cleaved front is offered to the fluid. If there is no mass transport necessary, a steady-state growth velocity should be obtained [26].
(3) Heterogeneous nucleation and subsequent growth starting from a germ of prescribed structure.

Homogeneous nucleation requires an additional careful treatment of fluctuations (see again [20]) but is also contained in the framework of dynamical density functional theory. Incorporating a sheared situation into DDFT has not yet been done but is in principle possible.

4. Application of DDFT to gradual versus sudden solid heating

An example for how dynamical density functional theory works for freezing and melting is shown for a two-dimensional system interacting via an inverse power potential $u(x) = \epsilon/x^3$.† Here $x = \rho^{1/2}r$ denotes particle distance, where ρ is the average density. In this case reliable equilibrium functionals $F[\rho(\vec{r}, t)]$ are known [27, 28] which describe freezing in quantitative accordance with experiments [29].

Here, we use the approximation of Ramakrishnan and Yussouf [28] to the equilibrium density functional. Starting from an initial density profile $\rho_0(\vec{r}, t = 0)$, equation (1) is numerically solved for times $(t/\tau_B) \lesssim 100$, where $\tau_B = (\rho D)^{-1}$ is the Brownian time scale. In this case the rectangular periodic box with $L_x/L_y = \sqrt{3}$ comprises two solid particles. Due to lattice symmetry, it suffices to solve the problem in a single elementary cell.

As a first application, we study melting of a highly ordered two-dimensional, infinite triangular crystal which is in equilibrium for a low temperature $T_0 = 0.016\epsilon/k_B < T_m$, where $T_m \simeq 0.028\,\epsilon/k_B$ is the melting temperature, at higher temperatures.

In a first Gedanken experiment we adiabatically increase the temperature T, i.e. we increase the temperature by a small step, let the system equilibrate, increase the temperature again, etc. and we proceed like that until the crystal melts to the fluid state. In figure 3 we plot the amplitude of the so obtained equilibrium density peaks $\rho_a^*(T) = \rho_a(\vec{r} = \vec{R}; T)$, where $\vec{R}$ denotes a lattice vector and the subscript a refers to the adiabatic situation, and the difference in Helmholz free energy density $\Delta F(T)/N = F[\rho_a(\vec{r}; T), T]/N - F_l(T)/N$, where $F_l(T) = F[\rho(\vec{r}) = \rho, T]$ is the free energy of the fluid, and N is the number of particles, as a function of T. We find that for temperatures $T \leq T_o \simeq 0.033\,\epsilon/k_B$ the system remains crystalline but only for $T \leq T_m \simeq 0.028\,\epsilon/k_B$ is the free energy difference negative and thus the crystal in thermodynamic equilibrium. For $T_m < T < T_o$ the free energy difference is positive implying the crystal is metastable and therefore overheated as can be seen in figure 3. The system is not able to overcome the free energy barrier which would lead to a favourable liquid state. For $T > T_o$ the crystal immediately melts into the fluid state.

In order to see whether the system upon increasing the temperature is able to circumvent the free energy barrier by choosing a different pathway through the free energy landscape we perform a second Gedanken experiment: starting from the same initial density profile $\rho_0(\vec{r}, t = 0)$ as above we heat the system instantaneously to a temperature $T_q > T_o$ and monitor the time evolution of the density profile $\rho_q(\vec{r}, t)$ where the subscript q refers to the quenched situation. In figure 4 we plot the amplitude of the density peaks $\rho_q^*(t; T_q) = \rho_q(\vec{r} = \vec{R}, t; T_q)$ for different quench temperatures T_q as a function of time. We find that the system reaches the same density profiles as above, i.e. $\rho_q(\vec{r}, t \to \infty; T_q) = \rho_a(\vec{r}; T_q)$. Therefore we conclude that upon heating the system, the heating rate does not affect the final density profile $\rho(\vec{r}, t \to \infty; T)$. Practically the same melting temperature is obtained for rapid or slow heating and thus overheating is retained.

---

† In three dimensions a similar study can be performed including solids and crystalline defects.
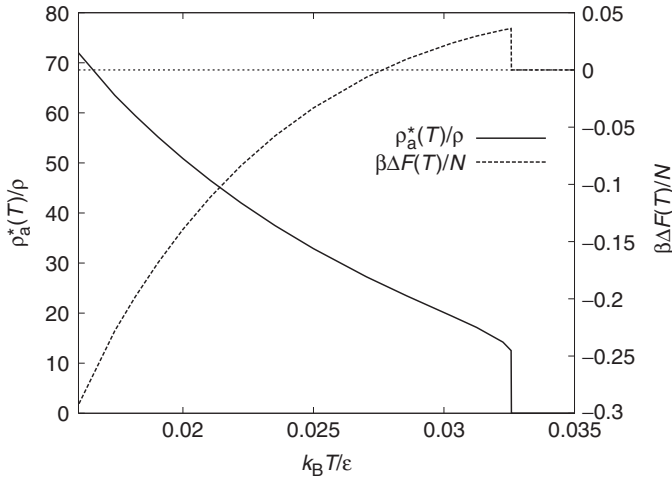
Figure 3. Height of the peak $\rho_a^\star(T)/\rho = \rho_a(\vec{r} = \vec{R}; T)/\rho$ and difference in free energy $\beta\Delta F(T)/N = \beta F[\rho_a(\vec{r}; T), T]/N - \beta F_l(T)/N$ as a function of $k_B T/\epsilon$ during an adiabatic temperature increase from $T_0 = 0.016\,\epsilon/k_B$.
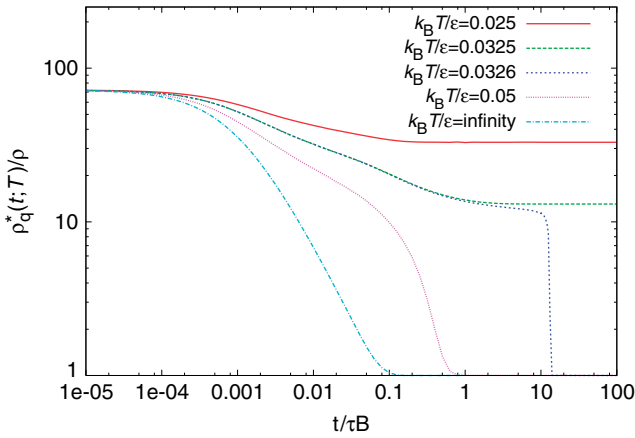

Figure 4. Height of the peak $\rho_q^\star(t; T)/\rho = \rho_q(\vec{r} = \vec{R}, t; T_q)/\rho$ as a function of time t/τ_B after a temperature quench to different temperatures T at time $t = 0$.

5. Relation to phase-field models

Phase-field models are derived on a more phenomenological (coarse-grained) level for order-parameter dynamics [30]. The resulting equations for the dynamics of the order parameter are similar to equation (1) if the corresponding functional is replaced by a square-gradient functional of the order parameter in the spirit of Ginzburg–Landau theory. These dynamical equations of the phase-field model are then solved numerically. There are numerous applications of phase-field dynamics to various circumstances of crystal growth and nucleation [31, 32].

   Phase-field models have been refined to incorporate more microscopic information from the solid phase. One important development in this direction is the description of the so-called phase-field crystal by suitable order parameters [33]. The phase-field crystal approach can also be generalized to include elastic distortions in the growing solid phase [34–37]. Dynamical density functional theory, on the other hand, operates on the full microscopic level without any phenomenological parameters. It is a challenge to derive the phase-field model from dynamical density functional theory. Then one should get insight into the levels of different approximations which are included in the phase-field approach (including the phase-field crystal). For the static density functional theory this has been performed [38, 39], but the extension towards dynamical situations is still missing.

6. Conclusions

In conclusion, computer simulations and dynamical density functional theory are ideal tools to study nucleation on a microscopic level, i.e. on molecular length and time scales. In particular, dynamical density function theory which is still in its infancy as far as applications of crystallization is concerned is expected to play a major role as a microscopic theory for any crystallization and nucleation event. One major effort will be to include properly the hydrodynamic interactions. At the same time real-space experiments on colloidal suspensions will give direct insight into the birth and growth of crystals such that mutual cross-fertilization of experiment, simulation and theory is expected in this research area [40].

References

 [1] D.W. Oxtoby, Nature **406** 464 (2000).
 [2] S. Auer and D. Frenkel, Adv. Polym. Sci. **173** 149 (2005).
 [3] U. Gasser, E.R. Weeks, A. Schofield, *et al.*, Science **292** 258 (2001).
 [4] U.M.B. Marconi and P. Tarazona, J. Chem. Phys. **110** 8032 (1999).
 [5] U.M.B. Marconi and P. Tarazona, J. Phys.: Condens. Matt. **12** A413 (2000).
 [6] H. Löwen, Phys. Rep. **237** 249 (1994).
 [7] D.L.J. Vossen and A. van Blaaderen, to be published.
 [8] R. Blaak, S. Auer, D. Frenkel, *et al.*, Phys. Rev. Lett. **93** 068303 (2004).
 [9] R. Blaak, S. Auer, D. Frenkel, *et al.*, J. Phys.: Condens. Matt. **16** S3873 (2004).
[10] R. Blaak and H. Löwen, Comput. Phys. Commun. **169** 64 (2005).
[11] T. Palberg, W. Mönch, J. Schwarz, *et al.*, J. Chem. Phys. **102** 5082 (1995).
[12] H.J. Schöpe and T. Palberg, J. Phys.: Condens. Matt. **14** 11573 (2002).
[13] P. Holmqvist, M.P. Lettinga, J. Buitenhuis, *et al.*, Langmuir **21** 10976 (2005).
[14] I. Cohen, T.G. Mason and D.A. Weitz, Phys. Rev. Lett. **93** 046001 (2004).
[15] I. Cohen, I.B. Davidovitch, A.B. Schofield, *et al.*, Phys. Rev. Lett. **97** 046001 (2004).
[16] D. Derks, H. Wisman, A. van Blaaderen, *et al.*, J. Phys.: Condens. Matt. **16** S3917 (2004).
[17] R. Evans, Adv. Phys. **28** 143 (1979).
[18] Y. Singh, Phys. Rep. **207** 351 (1991).
[19] A. Archer and R. Evans, J. Chem. Phys. **121** 4246 (2004).
[20] A. Archer and M. Rauscher, J. Phys. A: General **37** 9325 (2004).

[21] G. Chan and R. Finken, Phys. Rev. Lett. **94** 183001 (2005).
[22] A. Archer, J. Phys.: Condens. Matt. **18** 5617 (2006).
[23] M. Rex, C.N. Likos and H. Löwen, Phys. Rev. E **72** 021404 (2005).
[24] M. Rex, C.N. Likos, H. Löwen, *et al.*, Mol. Phys. **104** 527 (2006).
[25] J. Dzubiella and C.N. Likos, J. Phys.: Condens. Matt. **15** L147 (2003).
[26] S. van Teeffelen, C.N. Likos and H. Löwen, to be published.
[27] S. van Teeffelen, N. Hoffmann, C.N. Likos, *et al.*, Euro. Phys. Lett. **75** 583 (2006).
[28] T.V. Ramakrishnan and M. Yussouf, Phys. Rev. B **19** 2775 (1979).
[29] K. Zahn, R. Lenke and G. Maret, Phys. Rev. Lett. **82** 2721 (1999).
[30] H. Emmerich, *The Diffuse Interface Approach in Materials Science*, Lecture Notes in Physics M 73 (Springer, Heidelberg, 2003).
[31] H. Emmerich and R. Siquieri, J. Phys.: Condens. Matt. **18** 11121 (2006).
[32] L. Granasy, T. Pusztai and J.A. Warren, J. Phys.: Condens. Matt. **16** R1205 (2004).
[33] K.R. Elder, M. Katakowski, M. Haataja, *et al.*, Phys. Rev. E **88** 245701 (2002).
[34] K.R. Elder and M. Grant, Phys. Rev. E **70** 051605 (2004).
[35] N. Goldenfeld, B.P. Athreya and J.A. Danzig, Phys. Rev. E **72** 020601 (2005).
[36] C.V. Achim, M. Karttunen, K.R. Elder, *et al.*, Phys. Rev. E **74** 021104 (2006).
[37] P. Stefanovic, M. Haataja and N. Provatas, Phys. Rev. Lett. **96** 225504 (2006).
[38] H. Löwen, T. Beier and H. Wagner, Z. Phys. B **79** 109 (1990).
[39] J.F. Lutsko, Phys. Rev. E **74** 021603 (2006).
[40] H. Löwen, J. Phys.: Condens. Matt. **13** R415 (2001).